EFFECTS OF GAMMA RADIATION INDUCED FORCED FORMATION OF FREE RADICALS ON THE STRENGTH OF CONCRETE FOR USE IN NUCLEAR POWER PLANTS

by

Steven BURNHAM [1], Quentin FAURE [2], Michelle TAMPLIN [1], Long HUANG [3], and Tatjana JEVREMOVIC [1*]

[1] Utah Nuclear Engineering Program, The University of Utah, Salt Lake City, Ut., USA
[2] Special School for Public Works, Cachan, France
[3] Huntsman Cancer Institute, School of Medicine, The University of Utah, Ut., USA

In this paper, we present a summary of preliminary experiments and numerical assessments of the effects of gamma radiation induced formation of free radicals in the curing stage of concrete on its characteristics. Substantial literature reports on the damaging effects of long-term and high-dose gamma and neutron exposure on concrete. However, we show that short-term exposure of concrete to gamma radiation can be beneficial in increasing its compressive strength. The effects of exposing to 630 MBq ^{137}Cs the 56 cubes each made of 125 cm³ concrete during the first seven days of curing are compared to another 56 cubes cured by the conventional process. The average compressive strength of the gamma cured cubes is around 8.500 psi, while conventionally cured cubes show the lower average strength of around 6.700 psi. The microstructure of the gamma and conventionally cured concrete cubes is analyzed using a scanning electron microscope. The radiolysis within the microstructure of the concrete cubes is assessed with computational modeling based on Geant4. The production of free radicals from radiolysis is shown to increase with increasing source strength and increasing the time of exposure to gamma radiation. This research shows in general that curing concrete in gamma radiation field provides observable trends toward its increased strength.

Key words: concrete for nuclear industry, nuclear concrete strength, Geant4, gamma radiation

INTRODUCTION

About Concrete as Material: Concrete is a composite mixture of water, cement, and coarse and fine aggregates. Cement is a fine powdery material made primarily of limestone, acting as a binder to hold the concrete mixture together. Aggregates vary widely in composition and are locally dependent, for example they can be limestone or quartz based. All aggregates are generally smaller than 1.5 inches in size. Fine aggregates are generally classified as particles that pass through a 3/8-inch sieve. Aggregates account for 60-75 % of the total volume of a concrete mix, [1]. Cement absorbs water; when mixed with water a hydration process causes a formation of a gel known as Calcium-Silicate-Hydrate, or simply C-S-H [2]. The formation of C-S-H is highly amorphous and is represented by the general formula: $CaO_x SiO_2 H_2O_y$ where x and y both vary over a wide range with the calcium to silica, c/s, ratios typically between 1 and 2, [2]. Two common forms of C-S-H are the jennite mineral $Ca_9Si_6O_{18}(OH)_6 \, 8H_2O$, and tobermorite $Ca_5Si_6O_{16}(OH)_2 \, 4H_2O$. The formation of C-S-H gel gives a concrete its high compressive strength in serving as a link between the aggregates and the cement paste. The force of attraction between the cement paste is attributed to the Van der Waals forces [3]. Van der Waals forces are weak intermolecular attraction forces; the electron cloud of an atom can, by chance, become concentrated in one region of an atom or molecule, thus causing a momentary polarity of an atom. This can lead to a cascading effect where other nearby atoms or molecules experience a momentary polarity. The positively and negatively charged regions can then be attracted to each other. The resultant force of attraction is weak but taken together on a large scale the forces can combine to be significant [4]. The attraction is the result of positive and negative polarity of molecules.

Due to its versatility, concrete is the most commonly used construction material in the world [5]. As such, concrete is very widely used in the nuclear industry both as a building material as well as a radiation shielding material [6, 7]. For the current Generation II

---

* Corresponding author; e-mail: Tatjana.Jevremovic@utah.edu

fleet of the power reactors in operation, concrete is used for containment domes as well as biological shields. In the event of an accident, large containment structures made of concrete and steel are designed to reduce the radiation to the environment and reduce or stop the spread of fission products beyond the containment volume. The concrete integrity is therefore of paramount importance for continuous and sustained operation of nuclear power plants. For example, in the Crystal River Nuclear Power Plant, the concrete of the containment structure cracked on multiple occasions. This resulted in the premature closing of the nuclear power plant [8]. Newer reactors of the Generation III are built based on the Generation II technology but with improved efficiency and safety. As a result, concrete is heavily used for both biological shields and containment structures. The European Pressurized Water Reactor (EPR) uses additional concrete to protect the containment vessel. In the event of an accident, a layer of sacrificial concrete is used to catch a melting core and provide it with enough time to cool, thus protecting the overall containment structure [9, 10]. The Generation IV reactor [11-13] designs such as the sodium-cooled fast reactor, gas-cooled fast reactor, lead-cooled fast reactor, and supercritical water-cooled reactor are in various stages of the design phases [12, 14], in which concrete will still be used as a construction material for the reactor containment building and biological shields. Generation IV reactor designs have an increased focus on safety but will undoubtedly require robust containment structures in the event of a nuclear accident [13], and terrorism [15].

The main concrete property that measures the structural quality is its compressive strength. It depends on the water-to-cement ratio and the concrete curing time. Concrete compressive strength of commercial structures ranges between 3 000 and 12 000 psi while for the cast-in-place buildings, the strength usually ranges between 3 000 and 6 000 psi. The design criteria for compressive strength of concrete used in nuclear power plants' structures is defined in ACI 349-06 – Code Requirements for Nuclear Safety-Related Concrete Structures [16]. When concrete is exposed to extreme conditions such as chloride exposure, salt, or seawater, it must have a minimum compressive strength of 5 000 psi. Concrete that is exposed to less extreme environments can maintain a minimum strength of 4 000 psi[*].

The tensile strength of concrete is a measure of a structure's cracking under the load, and thus it is more important in designing highways and airfield slabs rather than a nuclear power plant's containment. It is usually defined to be 10-15 % of the compressive strength of concrete. For this reason, tensile strength is most often neglected in structural concrete building designs [16]. Reinforcing steel is used within concrete

---

[*]1 psi is one pound of force acting on one square inch; 1 psi is equivalent to 0.00689475729 MPa

structures in order to accommodate for the lack of tensile strength.

Concrete and radiation: There is substantial literature speaking of the damaging effects of radiation on concrete that is related to a long-term exposure of concrete to gamma and neutron irradiation in nuclear power plants. The most common elements in the concrete mix are Ca, Si, H, and O. In interacting with neutrons of low or high energies, the most probable interaction types are neutron elastic scattering and radiative capture. As a result, atoms (nuclei) in the solid lattice of concrete are dislocated; however, this defect will not accumulate in the cement portion of concrete mix due to its original imperfect crystalline structure. However, dislocation of atoms in aggregates will accumulate and can cause expansion that is the reason for observed cracks in the concrete structure. This in turn affects the strength of concrete. Therefore, concrete's resistance to neutron radiation decreases with a decrease of concrete aggregates resistance to neutron exposure. It is shown in numerous studies that neutron radiation with a fluence over 10^{19} ncm^{-2} may cause a noticeable increase in its volume, and therefore reduce concrete compressive strength. Due to specifics of neutron interactions with various nuclei in the concrete mix, an overall resistance of concrete to neutron radiation strongly depends on concrete mix proportions, type of a cement, and type of aggregates.

The lattice structure of the many different elements present in concrete is disordered due to gamma and neutron interactions in increasing concrete susceptibility to alkali silica reactions (ASR). Traditionally, aggregates in concrete that contain reactive silica will react with the highly alkaline environment of hydrating cement. This causes the aggregate to swell and in turn generates internal pressure within the concrete that can cause severe degradation [2]. In general, the radiation damage of the crystal lattice of otherwise unreactive aggregates has been shown to cause them to become reactive and induce ASR [17]. In order for radiation to cause damage in concrete in a measurable degree, high radiation doses of 10^7-10^{11} Gy of absorbed dose are found to be necessary [17, 18]. Therefore, the ASR can severely degrade the concrete and decrease its compressive strength.

Interaction of gamma rays or neutrons with elements in any media will result in energy transfer and therefore generation of heat. It has been previously shown that radiation can lead to an increase in temperature of an interacting medium as high as 250 °C while the threshold for degradation of concrete is only 95 °C [19].

Of interest to this paper is how gamma ray interactions with concrete can be beneficial when exposed to concrete during its initial curing time. This is of particular interest because high-dose exposure of concrete to gamma radiation is a known degradation mechanism, especially when exposed over decades

time. Little is known about the short-term effects of radiation on concrete and as is described in the following sections, short-term exposure may be able to provide positive benefits. The following section summarizes the main effects of gamma rays in interacting with concrete, and next one describes our experimental data on the effects of gamma rays on the curing concrete.

EFFECTS OF GAMMA RAYS IRRADIATION ON CONCRETE CHARACTERISTICS

Effects of gamma rays induced radiolysis of water on concrete

Literature indicates that long-term exposure to gamma (and/or neutron) irradiation reduces both tensile and compressive strengths as well as the modulus of elasticity of concrete structures of nuclear power installations. Specifically, a gamma dose on the order of 10^8 Gy may cause a reduction in concrete compressive strength. The most important interaction is with water in concrete that produces water radiolysis in cement paste. A consequence of this process likely causes the creep and shrinkage of concrete. As much as shrinkage is detrimental to matured concrete structures, we show in this paper that it has an incremental advantage if induced during the early development (curing) of concrete. In other words, the experimental results provided in the next section show gamma ray induced radiolysis of water during the early curing of concrete showing the overall strength of the curing concrete may increase. The potential heating caused by these interactions show no effects to the formation of concrete and therefore its strength.

In general, a response of any composite (mixture) material to irradiation directly depends on the responses of their components. Similarly, resistance of concrete to irradiation of any type (most important are gamma and neutron irradiation) depends directly on the resistance of the concrete's components. The most important is the effect of gamma interactions with water causing it to be decomposed by radiolysis into hydrogen and hydrogen peroxide, which in turn decompose into water and oxygen. The initial radiolytic step is described with [20]

$$H_2O \xrightarrow{\text{ionizing radiation}} e_{aq}^- {}^*,$$
$$HO, H, HO_2, H_3O^+, OH^-, H_2O_2, H_2 \qquad (1)$$
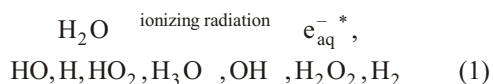
These complex species formed within concrete pores interact with themselves as well as with the elements present in aqueous solution of cement and water. Many of the products can react with each other

---

*The term e_{aq}^- refers to the initial free electron produced through the interaction of a gamma ray with a water molecule. This electron is captured by a water molecule and becomes solvated, being referred to as an aqueous or solvated electron. The solvated electron can react with H^+ to form the hydroxyl radical [21].
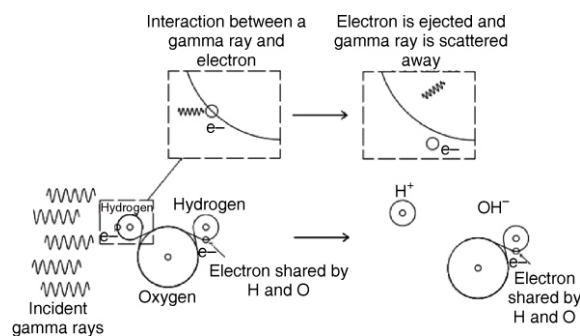

Figure 1. Scenario in which H^+ and OH^- are formed from Compton scattering of a gamma ray with a water molecule in concrete mixture

causing recombination back to water known as back reactions. The process of radiolysis can also create products such as hydroxide that are found in Tobermorite and Jennite, two forms of C-S-H. The radiolysis of water in concrete leads to the formation of free radicals that are formed in small clusters, the spatial distribution of which is characteristic of the energy of the ionizing radiation [22]. For example, gamma induced low-energy electrons in concrete form radicals at high concentrations along a travel track. High-energy electrons form regions of low radical density. The low density allows for the radicals to diffuse and react with solutes in water [22]. In the case of concrete, they react with Ca or Si that are in the solution, thus forming these products of hydration. One scenario explaining a creation of free radicals in concrete is illustrated in fig. 1.

Effects of gamma rays induced heating on concrete

Exposure of concrete to heat is categorized in three fundamental ways: effects on the hydrated cement paste, effects on the aggregates, and effects on the concrete as a whole. Cement mixed with water leads to the so-called hydration process that creates the products such as C-S-H. As it forms, it traps a free water and forms capillary voids. When concrete is subjected to heat, the C-S-H begins to release that water. In a concrete that is porous, the formed steam is released from its pores. In a concrete that is denser, this formed steam has no place to go and therefore results in the formation of an internal spalling, weakening the internal structure. Very high temperatures are required to dehydrate the C-S-H. For example, at temperatures of 500 °C, the C-S-H begins to dehydrate and decompose with its full decomposition starting at around 900 °C [3]. Hydration of cement is an exothermic reaction producing up to 500 Jg^{-1} cement [23]. In most instances, the heat is able to be transferred to its surroundings. Large concrete structures can present challenges due to the low thermal conductivity of concrete. It can act as an insulator and the interior body of the concrete can see a rise in temperature greater

310

S. Burnham, *et al.*: Effects of Gamma Radiation Induced Forced Formation of ...
Nuclear Technology & Radiation Protection: Year 2017, Vol. 32, No. 4, pp. 307-319

than 55 °C [23, 24]. Instances where there is a large increase in temperature can cause the concrete to expand and then contract non-uniformly, causing premature cracking and internal stresses [24]. The heat of hydration can be mitigated by slowing the hydration process and allowing for dissipation of heat. This is accomplished using the so-called set-retarding admixtures [3]. Accelerating the hydration process too much, however, can cause excessive internal heating even in small structures that might not otherwise be affected by the heat of hydration.

The effects of heat on the aggregates in concrete are similar to hydrated cement paste. Porous aggregates have their water converted to steam. In a low porosity environment, the steam will create internal pressure and cause the aggregate to crack and lose strength. Other specific types of aggregate can have varying effects. Granite and sandstone that are high in silica will undergo a phase change at 573 °C that causes sudden expansion [3]. An expansion of aggregate causes increased pressure within the entire concrete structure forming cracks. The cracks will weaken the bond between the aggregate and hydrated cement, thus decreasing compressive strength.

The effects of heating on both the hydrated cement and aggregate combine to affect concrete in a negative manner. It was demonstrated [25] that concrete exposed to temperatures over 800 °C for even a short duration of time can reduce 40 % of its strength.

Radiation heating of concrete can also have negative effects in the form of both shrinkage and expansion [26]. As stated earlier, when the hydrated C-S-H is heated, the internal water is released in the form of steam. This process causes the C-S-H to lose its volume. On the other hand, the aggregate can expand as a result of its lack of porosity not allowing the water to escape as easily. Larger aggregate sizes create a mismatch in size with the shrinking C-S-H resulting in less surface area contact and decreasing the overall strength on the concrete mix.

The amount of heating generated due to gamma rays interaction with any material can be approximated by taking into account the energy absorbed by the material (absorbed dose) and the specific heat capacity of the material, as follows [27]

$$Q = c\Delta T \qquad (2)$$

where Q is the energy absorbed or absorbed radiation dose by a material [Jg^{-1}], c – the specific heat capacity of a material or the energy required to raise the temperature by 1 °C [1 Jg^{-1} °C^{-1}] for fresh concrete, determined experimentally [28]), and ΔT – the change in temperature of the material absorbing radiation [°C].

For example, if a fresh concrete mixture is exposed for seven days to a ^{137}Cs source of intensity of 630 MBq, corresponding to absorbed dose of 0.746 Jkg^{-1}, it follows that increase in concrete internal temperature due to gamma ray interactions is negligible

$$\Delta T = \frac{7.46 \cdot 10^{-4} Jg^{-1}}{1Jg^{-1} \, °C^{-1}} = 7.46 \cdot 10^{-4} \, °C \qquad (3)$$

EFFECTS OF GAMMA RADIATION ON CONCRETE CHARACTERISTICS DURING ITS EARLY STAGE OF CURING

This section describes the experiment we have developed to assess if the curing concrete exposed to gamma rays develops with enhanced strength and to understand what processes may be responsible for such a finding.

Experimental set-up to gamma curing process

Based on the process of radiolysis of water within concrete as well as on understanding some of the known structures of C-S-H gel, we explored the possibility that short-term exposure of concrete to gamma radiation can enhance the curing phase and lead to its increased strength. In the experiment, we exposed curing concrete in a controlled environment (temperature and humidity) to a ^{137}Cs source for the first seven days after it was mixed. The concrete mixtures were controlled to ensure consistency among the concrete cubes within accepted laboratory practices. The experiment included as follows.

– Measuring the absorbed radiation dose to concrete cubes exposed to a 630 MBq ^{137}Cs source for seven days. A ^{137}Cs source was chosen because it is a mono-energetic source emitting a single 662 keV gamma ray. The activity of 630 MBq was chosen based on source availability in our laboratory and it has been chosen to not neither be too weak nor be too strong.

– Measuring the compressive strength of gamma cured *vs.* conventionally cured concrete after seven days of curing.

– Analyzing the changes in the microstructure of concrete cubes in relation to the measured compressive strength.

– Analyzing if gamma heating causes any micro or macro structural changes within the concrete cubes.

– Determining the rate at which free radicals are produced within the micro pores of concrete and their correlation to concrete strength.

Several batches of the same concrete mixture were developed in the laboratory of the Utah Nuclear Engineering Program during the months of February and March, 2016 with the following content: 0.4 water to cement (w/c) ratio with only fine aggregates (sand) mixed in a 2.75 sand to cement (s/c) ratio. Procedure for mixing the concrete cubes is outlined in ASTM Standard C192/192M – Making and Curing Concrete

S. Burnham, *et al.*: Effects of Gamma Radiation Induced Forced Formation of ...
Nuclear Technology & Radiation Protection: Year 2017, Vol. 32, No. 4, pp. 307-319

311

Test Specimens in the Laboratory [29]. Due to the fineness of the aggregates used, concrete cubes of 125 cm^3 in volume are cast and used for the compressive strength testing. The ASTM C192/192m procedure is followed, but concrete cubes are demolded after only five hours of curing time, because we were testing the effects of gamma radiation on concrete during the very early stages of curing. Therefore, the test cubes were demolded as soon as they were able to hold their form on their own and thus be placed in the gamma irradiator. After demolding, both sets of concrete cubes are cured in dry air for a period of seven days. One set was exposed to a 630 MBq source during the entirety of the seven days while the other set of concrete cubes was not exposed to any radiation other than naturally occurring background radiation.

Although preliminary analytic estimates show that exposure of concrete to 630 MBq ^{137}Cs source for seven days will not generate any excess heat within the concrete, we also examined if gamma heating would be generated in the concrete cubes in any observable way and compared it to the effects that heat may produce as follows: one set of cubes was cured in dry air and exposed to the same 630 MBq source, while the second set was cured in dry air with no exposure to this same source. Additionally, a third and fourth set of cubes were cured in an oven: one set at 95 °C and the other at 120 °C.

Gamma rays absorbed dose within the concrete cubes: experimentally measured and MCNP6 estimated

The absorbed dose due to gamma ray interactions within the concrete cubes was both calculated and determined experimentally.

The exact experiment layout is shown in fig. 2(a), while the MCNP6 model of the experiment is shown in fig. 2(b). As can be seen, the isotropic ^{137}Cs source with gamma energy of 662 keV is placed in the center of the twelve 125 cm^3 volume concrete cubes.

MCNP6 values: In general, when using MCNP6 (Monte Carlo N-Particle) [30], the absorbed radiation dose is calculated using the F6 tally and confirmed us-
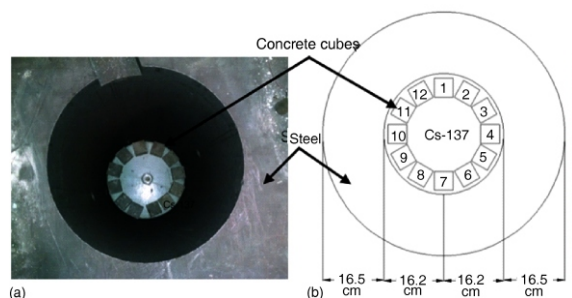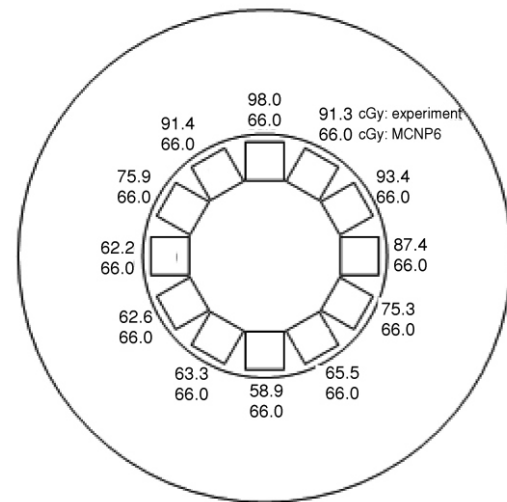

Figure 3. Experimental and MCNP6 absorbed dose values due to gamma exposure to concrete cubes (the MCNP6 calculated absorbed dose for each cube is the same because the ^{137}Cs isotropic source is placed exactly in the center of all the concrete cubes. In the experimental set-up the source was not located as precisely at the center as in the MCNP6 model thus the values of the absorbed dose vary)

ing the *F8 tally. The absorbed dose is obtained to be 66 cGy for cement cubes as well as the sand and cement cubes when exposed to a ^{137}Cs 630 MBq source for seven days with an error of 0.3 %. The *F8 tally yields results that are within 0.2 % of the F6 tally (65.9 cGy) with an uncertainty of 0.3 %. Figure 3 shows the absorbed dose map, based on calculated and measured values. It can be seen that the calculated dose is the same for every concrete cube. This is because the MCNP6 geometry is perfectly symmetrical, the isotropic ^{137}Cs source is located exactly in the center with all cubes located at the exact same distance from it. In the experiment, however the position of the source is subject to change as it is used in other tests and experiments. It is however, placed as close to center as possible before each experiment. The MCNP6 model therefore presents an average value expected across all future experiments and the discrepancy in the dose values for the experiment is therefore expected (as explained below).

Experimental values: A Landauer nanoDOT [31] system is used to measure the absorbed dose in the concrete cubes fig. 2(a). The nanoDot system is known to have a linear response up to 3 Gy of exposure and is accurate to within 5 % for an energy range of 5 keV to 20 MeV [31]. The nanoDots used in this experiment were previously used and therefore were irradiated but had only accumulated a dose of 1.5 Gy or less. The low dose accumulation provided assurance that they will be suitable for further use since the total cumulative dose will not exceed 3 Gy. The linear response of the nanoDots was verified by exposing three nanoDots to 1 Gy from a 6 MV X-ray source. An additional three nanoDots were also exposed to a dose of

Figure 2. Experimental set-up (a) for gamma curing and MCNP6 model (b) for calculating absorbed gamma ray dose to concrete cubes

312

S. Burnham, *et al.*: Effects of Gamma Radiation Induced Forced Formation of ...
Nuclear Technology & Radiation Protection: Year 2017, Vol. 32, No. 4, pp. 307-319

Figure 4. Experimental measurement of the cumulative radiation dose response of Landauer nanoDots with a 6 MV X-ray source
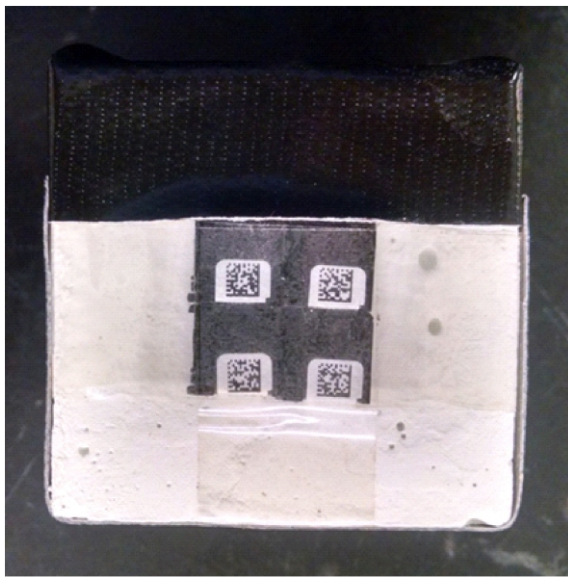

Figure 5. Concrete cube with nanoDots placed on the front face for dose measurement from exposure to ^{137}Cs source

2 Gy from the same 6 MV X-ray source. The experiment layout is shown in fig. 4. The total cumulative dose is then measured to test the linear response and accuracy of the measurement when the nanoDots are re-used. Two nanoDots are placed on the front and back of each of the concrete cubes prior to exposure to the ^{137}Cs source. The measured dose of the nanoDots indicated that the dose response was linear as expected and accurate, making the nanoDots suitable for re-use. The dose response is then tested by exposing the nanoDots to the 630 MBq ^{137}Cs source. Four nanoDots with accumulated dose from previous experiments were placed on the front of a concrete cube as shown in fig. 5. The dose to each of the nanoDots is measured and the initial dose is subtracted from the total cumulative dose to determine the total exposure to each of the nanoDots. The average absorbed dose was 74.6 cGy. Table 1 shows the measured dose values for each of the nanoDots. The measured dose is also compared to the MCNP6 calculated dose of 66 cGy. Table 1 shows that the nanoDots responded correctly after

Table 1. Absorbed dose of four nanoDots from exposure to ^{137}Cs source

nanoDot	Starting dose [cGy]	Measured cumulative dose [cGy]	Measured cumulative dose – starting dose [cGy]
1	112.733	186.119	73.385
2	84.756	159.043	74.287
3	120.163	192.648	72.485
4	149.549	227.861	78.312

exposure to a 630 MBq ^{137}Cs source for seven days making them accurately suitable for the use in this experiment.

The absorbed dose was measured for two different concrete cube mixes: the first consisting of six cubes made of only water and cement (cement paste) at a proportion of 0.4 w/c as stated earlier, and the second consisting of six cubes where sand was added at a ratio of 2.75 s/c. On each of the twelve cubes, two nanoDots are placed at the side directly facing the ^{137}Cs source and two are placed on the rear face directly opposite, shown in fig. 6. After seven days of exposure, the dose to each of the nanoDots was measured. The dose of each nanoDot on the rear face was subtracted from the measured dose of the nanoDot on

Figure 6. Concrete cube with two nanoDots for absorbed dose measurement

Table 2. Measured absorbed dose in cement paste cubes and sand and cement cubes

Mixture	Cube	Front cube dose [cGy]	Back cube dose [cGy]	Front cube dose minus back cube dose [cGy]
Cement paste	1	136.6	38.6	98.0
	2	127.2	35.9	91.3
	3	125.7	32.2	93.4
	4	120.0	32.6	87.4
	5	103.4	28.1	75.3
	6	94.7	29.3	65.5
Sand and cement	7	85.1	26.2	58.9
	8	89.2	25.8	63.3
	9	90.0	27.4	62.6
	10	91.6	29.5	62.2
	11	106.0	30.1	75.9
	12	124.4	33.0	91.4

the front face of the concrete cubes to obtain the total dose absorbed by the concrete cubes itself.

Cubes 1, 2, and 3 (see fig. 3) received absorbed doses higher than cubes 4, 5, and 6. This is explained by the slightly off-center position of the ^{137}Cs source, making it closer to cubes 1, 2, and 3 and further away from cubes 4, 5, and 6. Cubes 5-10 most closely match the distance of the ^{137}Cs source in the MCNP6 simulation of 11 cm. This is reflected in that they also most closely match the calculated dose rates shown in fig. 3. Those cubes that were closer to the source as a result of it being placed slightly off center had higher absorbed dose rates. The average absorbed dose to the sand and cement cubes is found to be 69.1 cGy while the average of the cement cubes is found to be 85.5 cGy. These values are compared to an MCNP6 calculated value of 66 cGy. The sand and cement cubes (7-12) are generally closer to the 11 cm distance of the source in the MCNP6 model while the cement cubes (1-6) are even closer to the source causing a higher average absorbed dose. The absorbed dose values for all 12 cubes are shown in tab. 2.

Comparison of compressive strength between the gamma cured and conventionally cured concrete cubes

Compressive strength testing is performed on only the sand and cement cubes according to the proportions and time frame outlined erlier. The sand and cement mixtures more accurately represent the concrete mixtures used in construction. The cubes that were used in the dose measurement experiment were not tested for compressive strength. During the placement and removal of the nanoDots, the cubes became too damaged to accurately test for compressive strength. As a result, a total of 120 concrete cubes from five separate batches of concrete cube mixes are tested for compressive strength. Each batch consisted of 12 cubes marked for gamma curing and 12 cubes marked

for conventionally curing. Occasionally, a few cubes from each batch would stick to the molding and become damaged in such a way that they had to be discarded. This occurred in batches 4 and 5 of both the gamma cured and conventionally cured cubes. In total, 112 cubes were tested for compressive strength. Half of the cubes (56) are gamma cured while the other half are conventionally cured. Compressive strength testing is performed in the University of Utah Structures Laboratory using an INSTRON universal testing machine [32] with computer controlled loading rate. All testing is performed in accordance with ASTM standard C109 – *Standard Test Method for Compressive Strength of Hydraulic Cement Mortars* [33]. Each of the cubes is loaded into the INSTRON machine applying a loading rate of 200 lb/s in accordance with ASTM C109. The compressive strength of each cube is shown in fig. 7.

The average compressive strength of the gamma cured concrete is 8 563 psi while the average compressive strength of the conventionally cured concrete is 6 710 psi. A *t*-test* is performed to compare the gamma cured cubes to the conventionally cured cubes in order to analyze the closeness of the two data sets. The resultant *p*-value** from the *t*-test is $1.26 \cdot 10^{-12}$, indicating that the two data sets are dissimilar and the overall compressive strength of the gamma cured concrete is
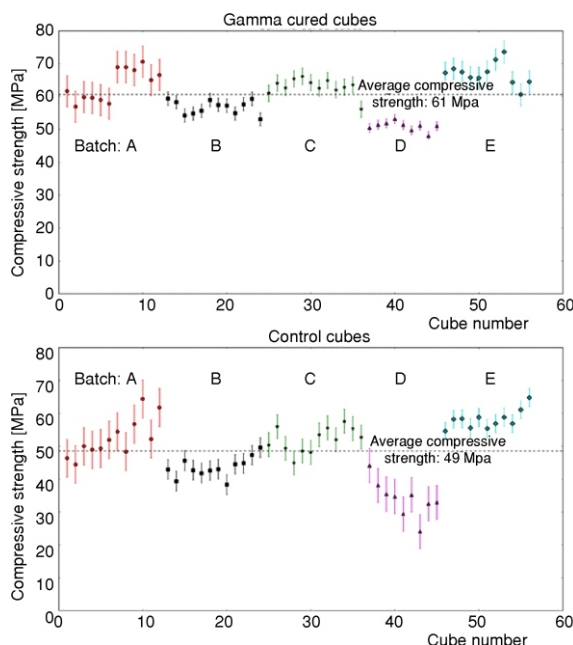

Figure 7. Compressive strength of gamma cured (top) and conventionally cured (bottom) concrete cubes. The five batches labeled A-E are mixed between the months of February-March, 2016

---

* A *t*-test is a statistical test used to compare different sets of data in order to determine if they are the same or significantly different from each other.
** The *p*-value represents the probability from the t-test that the two data sets being compared are the same

314

S. Burnham, *et al.*: Effects of Gamma Radiation Induced Forced Formation of ...
Nuclear Technology & Radiation Protection: Year 2017, Vol. 32, No. 4, pp. 307-319

higher than the conventionally cured cubes. The gamma cured cubes also exhibited a lower average standard deviation (405.4 psi) compared to the conventionally cured cubes (592.04), indicating greater consistency in each of the batches when gamma cured. The only exception is batch E where the gamma cured had a standard deviation of 481 psi while the conventionally cured had a standard deviation of 401 psi. The average compressive strength of batch E of the gamma cured (9 700 psi) is still higher than the average compressive strength of batch E of the conventionally cured (8 430 psi). It is anticipated that with more testing, the majority of the batches will follow the trend of having both a lower standard deviation and higher average compressive strength and that batch E will be shown to be an anomaly.

Analysis of the concrete cubes micro structure using the scanning electron microscope (SEM)

The crushed remains of the concrete cubes from batch *E* (11 gamma cured and 11 conventionally cured cubes) are collected and sealed in plastic bags after compressive strength testing for analysis using SEM. In the Crus Advanced Materials Technology Center at the University of Utah, a Hitachi S-4800 SEM is used to examine the microstructure of the concrete cubes in order to correlate the difference in their compressive strength values (batch E, as shown in fig. 7). The compressive strength of the gamma cured and conventionally cured cubes from batch E shown in fig. 7 are shown in greater details in fig. 8. The microstructure of the gamma cured concrete cube with the highest compressive strength of 10 662 psi, concrete cube 8 shown in fig. 8(a), and the microstructure of the conventionally cured concrete cube with the highest compressive strength of 9 396 psi, concrete cube 11 shown in fig. 8(b), is compared. The SEM images of these two cubes are shown in fig. 9. Both cubes are similar in showing a low void ratio. The void ratio is represented by the dark areas in the SEM images. A lower void ratio means that there is more contact between the C-S-H and the aggregate, causing an increase in strength.

The concrete cubes from batch E with the lowest compressive strength as shown in fig. 8 (gamma cured concrete cube 10 with compressive strength of 8 378 psi and conventionally cured concrete cube 1 with compressive strength of 7 528 psi) are also compared using the SEM and the images are shown in fig. 10. Both cubes show similar SEM images with a low void ratio and well-developed C-S-H.

From these SEM image analyses, it appears that the gamma and conventionally cured concrete are shown to be similar in their void ratios as well as their development of C-S-H for both the cubes with high and with low compressive strength. The analysis suggests that for
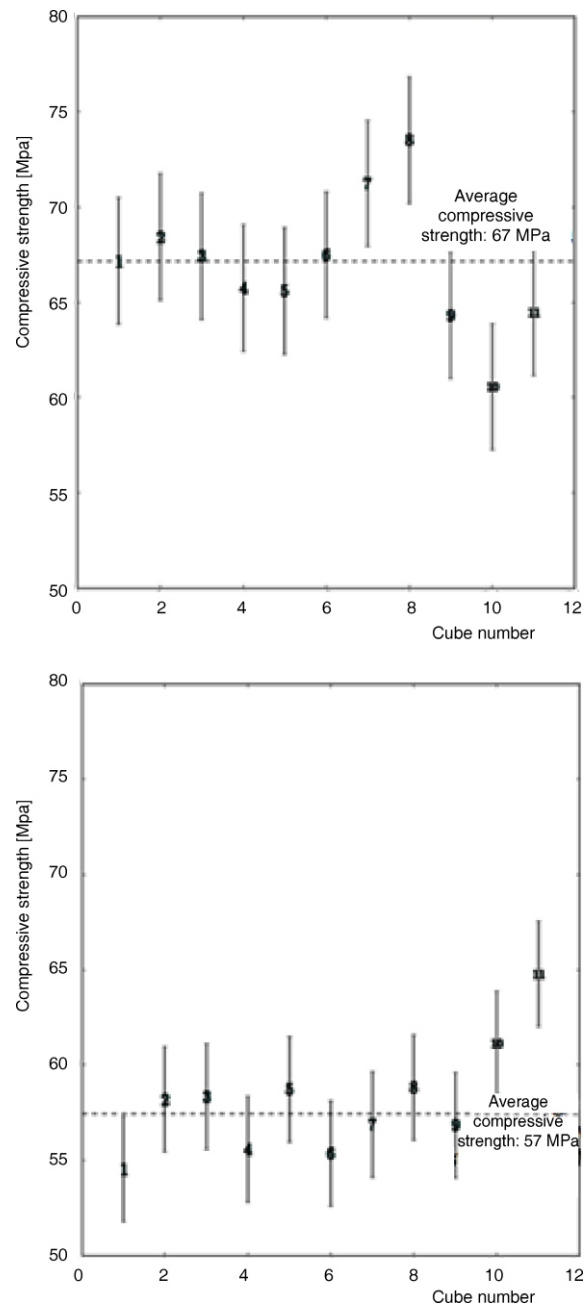

Figure 8. Detailed view of the compressive strength of batch E of (a) gamma cured and (b) conventionally cured concrete cubes (mixed on 8 March 2016)

short-term exposure to gamma radiation and absorbed gamma doses of less than 1 Gy (fig. 3), no significant or visible changes occur to the microstructure of concrete. The lack of change in the microstructure suggests that the increase in strength observed in the gamma cured cubes is likely due to changes occurring at the molecular level and interactions taking place between free radical formation and the products of hydration formed during the early curing stages. The complexity of C-S-H is not well understood [34]. The SEM analysis is only able to provide visual structure of the concrete at the micro level. Our future research, already on-going, is addressing this issue.

Figure 9. SEM images of (a) cube 8 of fig. 8(a) (gamma cured) and (b) cube 11 of fig. 8(b); (conventionally cured) concrete cubes with the highest compressive strength as shown in fig. 8
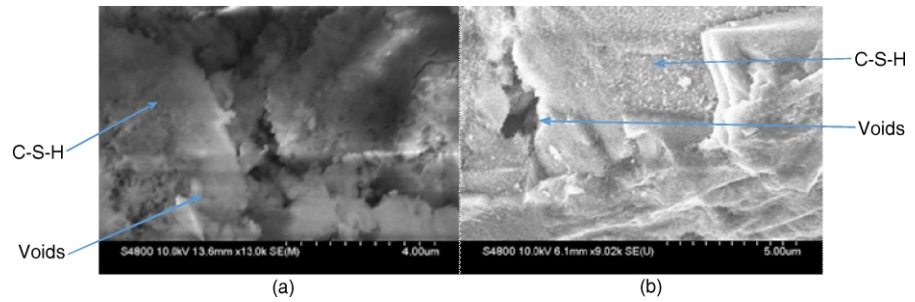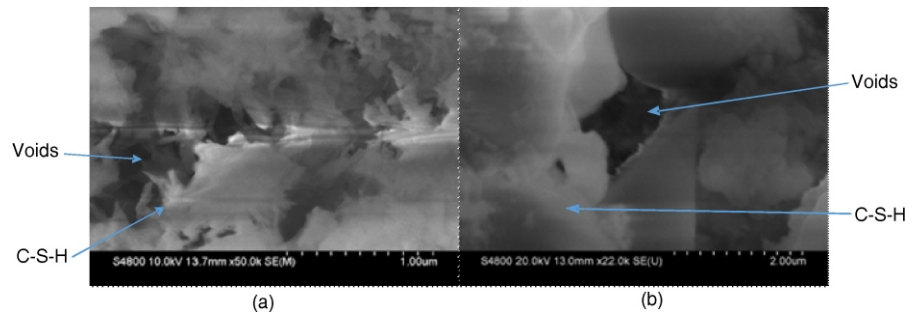

Figure 10. SEM images of (a) cube 10 of fig. 8(a) (gamma cured) and (b) cube 1 of fig. 8(b) (conventionally cured) concrete cubes with the lowest compressive strength as shown in fig. 8

Effects of gamma rays induced heating on concrete microstructure

Gamma radiation cured concrete cubes are also compared to cubes that are cured in a high temperature environment in order to assess if the analytical estimates compared to the experiment. As described previously, heat can cause damage to concrete at temperatures as low as 95 °C. The same concrete mix as described in the Experimental set-up is used to analyze the effects of high temperature on the microstructure using SEM. The SEM images are then compared to those of the gamma cured cubes in order to compare if any gamma heating may be taking place. Twelve concrete cubes are cured using gamma radiation in the same manner as described in the experimental set-up. Eleven cubes are cured in an oven at 95 °C, while six (6) cubes are cured in the oven at 120 °C. The number of cubes in each batch is dependent on the number of concrete molds available in the laboratory at the time of mixing. The two temperatures were chosen based on a literature survey [19] indicating that the damage to concrete can occur at temperatures at and above 95 °C. A slightly higher temperature of 120 °C was also chosen since it is high enough above the boiling point of water that dehydration and steam formation within the pores is expected to be therefore accelerated. A batch of six (6) cubes is used as a control and they are cured in dry air at 23 °C with no exposure to radiation and are mixed according to the same standards as described in the Experimental set-up. All cubes are tested for compressive strength using the same method, and the crushed cubes are then saved for SEM analysis. The measured compressive strength is shown in fig. 11. The compressive strength of the gamma cured cubes is compared to the cubes cured in the

oven, and control cubes, using a *t*-test. The resultant p-values for the gamma cured compared to the heat cured concrete cubes at 95 °C, 12 °C, and the control at 23 °C are 0.025, 0.069, and 0.04, respectively. These *p*-values indicate that the gamma cured cubes still exhibit a higher overall compressive strength than those cured using heat or the control set.

The microstructure of the concrete cubes with the highest compressive strength from batches A, B, and C (fig. 11) are shown in fig. 12. These are cubes 6 (batch A, gamma cured), 1 (batch B, heat cured at 95 °C), and 1 (batch C, heat cured at 120 °C). The gamma cured and heat cured cube at 95 °C are nearly identical in appearance having small voids with well-developed C-S-H. The heat cured cube at 120 °C has C-S-H in similar appearance but has one large void that may be a result of greater dehydration due to the elevated temperature.

The cubes with the lowest compressive strength are also compared as shown in fig. 13. From fig. 11,
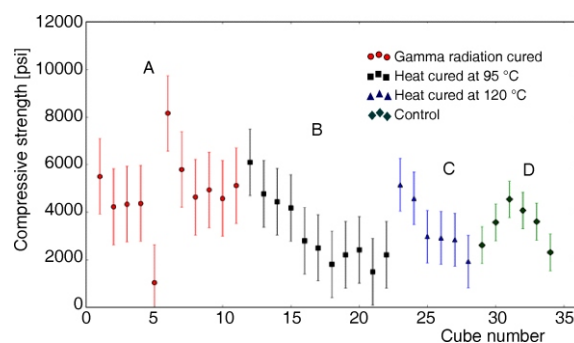

Figure 11. Compressive strength of gamma cured, heat cured cubes at 95 °C, heat cured cubes at 120 °C, and control concrete cubes. The control cubes were cured without any heat or gamma ray exposure

316

S. Burnham, *et al.*: Effects of Gamma Radiation Induced Forced Formation of ...
Nuclear Technology & Radiation Protection: Year 2017, Vol. 32, No. 4, pp. 307-319
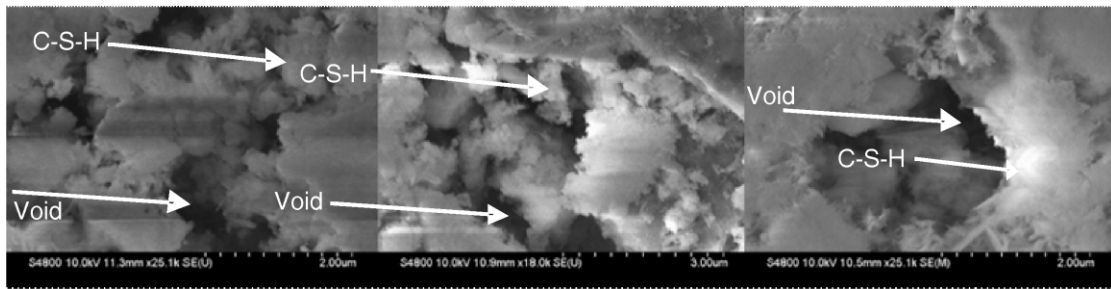
Figure 12. SEM images of (a) gamma cured concrete (cube 6 of batch A in fig. 11), (b) heat cured at 95 °C (cube 1 of batch B shown in fig. 11), and (c) heat cured at 120 °C (cube 1 of batch C shown in fig. 11). Each of these cubes has the highest compressive strength among the gamma cured ones, heat cured at 95 °C and heat cured at 120 °C as shown in fig. 11
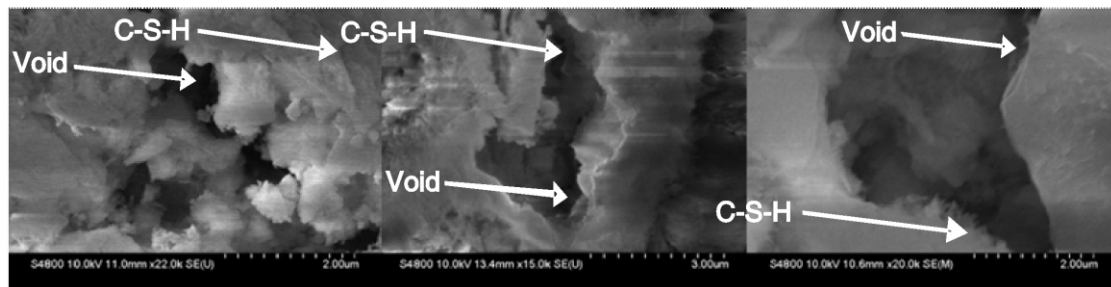

Figure 13. SEM images of (a) gamma cured concrete (cube 5 of batch A in fig. 11), (b) heat cured at 95 °C (cube 10 of batch B in fig. 11), and (c) heat cured at 120 °C (cube 6 of batch C in fig. 11). Each of these cubes has the lowest compressive strength among the gamma cured, heat cured at 95 °C and heat cured at 120 °C as shown in fig. 11

these are cubes 5, 10, and 6 for the gamma cured (batch A), heat cured at 95 °C (batch B), and heat cured at 120 °C (batch C), respectively. Similar to the cubes with the highest compressive strength, the gamma cured and heat cured at 95 °C exhibit comparable features with a low void ratio and well-developed C-S-H. The cube cured at 120 °C also has features similar to cube 1 which has the highest compressive strength as shown in fig. 13(c).

It was already shown that the gamma source used for this experiment does not cause any meaningful change in temperature in the concrete cubes. From the SEM analysis comparing gamma and heat cured concrete cubes, it is shown that even if heating is to occur to a degree that damage has been shown to occur [18] (>95 °C), seven days is not enough time to disrupt the microstructure within the concrete cubes.

Geant4 simulation of free radical formation within concrete

To better understand the radiolysis occurring within the micropores of the gamma cured concrete, Geant4 [35] is used to simulate the formation of free radicals as well as the rate at which they are formed. The *chem2* example provided in the Geant4-DNA toolkit [36, 37] is used as a base for this simulation. The *chem2* module simulates radiolysis and its associated reactions. The material definition of the world is defined as portland cement and water with a w/c ratio of 0.4. The composition for portland cement concrete for usage in

Geant4 is obtained from the Compendium of Material Composition Data for Radiation Transport Modeling [38]. Porosity is simulated by homogenously distributing water in a volume of portland cement. A porosity value of 14 % is used based on literature values for a 0.4 w/c mix ratio [39]. The geometry accurately replicates the laboratory experiment in fig. 2, a 125 cm^3 cube composed of cement and water and placed 11 cm from a ^{137}Cs source. The Geant4 model is shown in fig. 14. Three different source strengths of 37 MBq, 630 MBq, and 1 260 MBq with four different exposure times of one hour, twelve hours, one day, and seven days are simulated. The total production of free radicals in moles/s is shown in figs. 15-17.

The simulation shows that as both time of exposure and source strength increases, the production of free radicals also increases. Free radical production does, however, begin to taper off with increasing time and source strength. The difference between seven
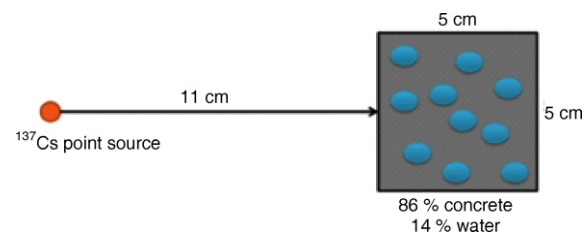

Figure 14. Geant4 simulation geometry of gamma rays from a ^{137}Cs source interacting with concrete and leading the formation of free radicals
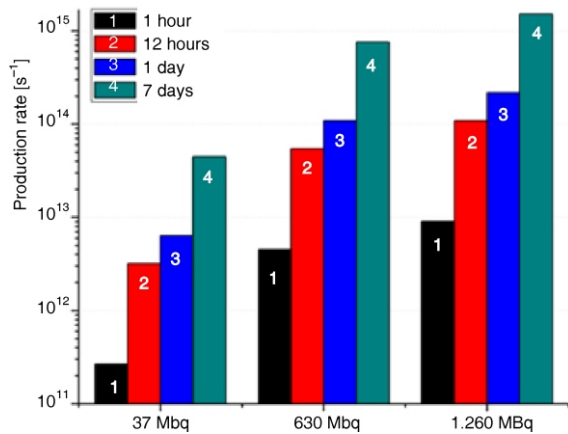
S. Burnham, *et al*.: Effects of Gamma Radiation Induced Forced Formation of ...
Nuclear Technology & Radiation Protection: Year 2017, Vol. 32, No. 4, pp. 307-319

317

Figure 15. Production of the H$_2$ radical within the micro pores of a 125 cm^3 sample of concrete in moles/s

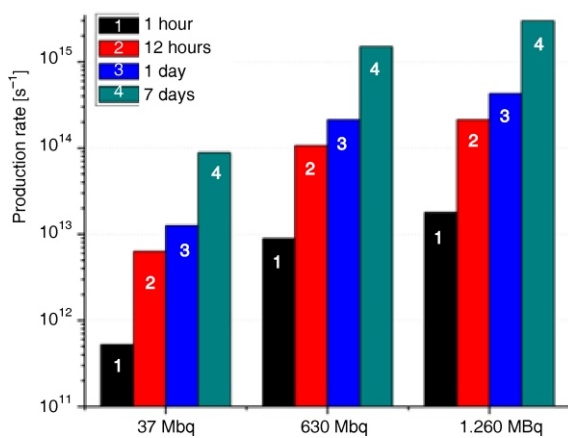**Figure 16. Production of OH$^-$ radical within the micro pores of a 125 cm^3 sample of concrete in moles/s**
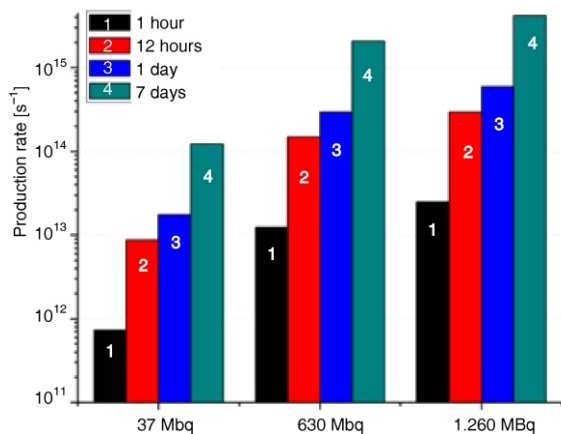

Figure 17. Production of H$_2$O$_2$ radical within the micro pores of a 125 cm^3 sample of concrete in moles/s

days of exposure at 630 MBq and 1260 MBq is not twice as much, despite the source strength being twice as strong. This suggests that the benefits of increased strength from gamma curing might also begin to taper off and a source twice as strong may not offer any increased benefit. The free radical production also begins to taper off with time of exposure. The results support the idea that gamma exposure is most beneficial

during the early stages of curing. For these reasons sources of lower and higher strength are not used in the experiment as the simulation shows the benefits would be minimal or non-existent.

CONCLUSIONS

Substantial literature documents how both gamma and neutron radiation have degrading effects on concrete over time periods of several decades of exposure. The C-S-H, a product of hydration within concrete, acts as a binder for all the concrete constituents. Radiation can cause heating within the internal concrete structure and cause the C-S-H to dehydrate and lose its strength. The process of dehydration from radiation can be caused by two mechanisms: gamma heating and radiolysis. Dehydration of C-S-H causes shrinkage and therefore a loss in volume. The shrinking C-S-H has less surface area to bond to aggregates, creating an overall decrease in overall strength of the concrete. Heat can also cause internal stress in aggregates as the water contained in their pores is converted to steam. The internal pressure causes cracking and a loss of strength. The structure of C-S-H can vary widely and exists in many forms such as Jennite and Tobermorite. When gamma rays interact with water, radiolysis will occur, forming free radicals such as H$^+$ and OH$^-$, the formation of which may be beneficial to concrete's compressive strength. We presented the results of short-term gamma radiation exposure to concrete during its first seven days of curing, and how its properties change. A 630 MBq ^{137}Cs source is shown to provide a calculated dose of 0.66 Gy and an average measured dose of 0.75 Gy to concrete cubes 125 cm^3 over seven days of exposure. The dose is calculated with the MCNP6 and determined experimentally. A slight difference between the calculated and experimental doses is due to the off-center positioning of the ^{137}Cs source in the experiment, causing a higher dose in some of the concrete cubes. The dose is substantially less than required to damage to concrete. The compressive strength of gamma cured and conventionally cured concrete cubes is compared showing that gamma cured cubes have an average compressive strength of 8563 psi compared to conventionally cured cubes with average compressive strength of 6710 psi. The gamma cured cubes also exhibited a lower standard deviation than the conventionally cured cubes. The SEM analysis of the microstructure of the gamma and conventionally cured cubes yielded no discernable difference between the two, suggesting that changes most likely are taking place at the atomistic level. A possible explanation is the process of radiolysis that creates an excess of H$^+$ and OH$^-$ promoting formation of C-S-H more quickly. A more rapid formation of C-S-H thus may cause better bonding between the aggregates at an earlier stage of concrete curing. The formation of free radicals within the microstructure of concrete cubes was analyzed also with Geant4 computational modeling. Increasing

318

S. Burnham, *et al.*: Effects of Gamma Radiation Induced Forced Formation of ...
Nuclear Technology & Radiation Protection: Year 2017, Vol. 32, No. 4, pp. 307-319

source strength and time of exposure shows an increase in the rate of free radical productions. It is, however, shown that after seven days of exposure to 630 MBq gamma source, the increased rate of production is minimal. The results support the idea that the benefits of gamma curing are most beneficial during the first seven days of curing. Future testing is planned to include curing cubes for 28 days in comparison to conventionally cured concrete cubes, to analyze if the benefits do diminish over time. Additionally, molecular dynamics simulation of concrete under these conditions is underway.

ACKNOWLEDGEMENT

AUTHORS' CONTRIBUTIONS

S. Burnham performed all experiments, calculations, and analysis with the help of Q. Faure. M. Tamplin developed and performed Geant4 modeling and provided radiolysis reaction rates. L. Huang assisted with dose measurements using nanoDots system and provided the equipment to measure the nanoDots. T. Jevremovic supervised the presented research and development that resulted in this paper.

REFERENCES

[1] ***, Portland Cement Association, „Aggregates" 2015, [Online], Available: http://www.cement.org/cement-concrete-basics/concrete-materials/aggreates. [Accessed: 02-Aug-2016]

[2] Lea, F. F. M., Lea's Chemistry of Cement and Concrete, Butterworth-Heinemann, 2004

[3] Mehta, P. K., Monteiro, P. J. M., Concrete: Microstructure, Properties, and Materials, McGraw Hill Professional, 2013

[4] Petrucci, R. H., *et al.*, General Chemistry Principles and Modern Applications. Prentice Hall, 2010

[5] ***, Portland Cement Association, „Products", cement.org. [Online], Available: http://www.cement.org/cement-concrete-basics/products, [Accessed: 14-Jun-2016]

[6] Singh, V. P., Badiger, N, M., Investigation on Radiation Shielding Parameters of Ordinary, Heavy and super Heavy Concretes, *Nucl Technol Radiat, 29* (2014), 2, pp. 149-156

[7] Hadad, K., *et al.*, Enhanced Radiation Shielding with Galena Concrete, *Nucl Technol Radiat, 30* (2015), 1, pp. 70-74

[8] ***, Duke Energy Announces Closing of Crystal River Nuclear Power Plant, May 2013

[9] Fischer, M., The Severe Accident Mitigation Concept and the Design Measures for Core Melt Retention of the European Pressurized Reactor (EPR), *Nuclear Engineering and Design, 230* (2004), 1, pp. 169-180

[10] Bouteille, F., *et al.*, The EPR Overall Approach for Severe Accident Mitigation, *Nuclear Engineering and Design, 236* (2006), 14, pp. 1464-1470

[11] Ingersoll, D. T., Status of Physics and Safety Analyses for the Liquid-Salt-Cooled Very High-Temperature Reactor (LS-VHTR), Dec. 2005

[12] Hahn, D.-H., *et al.*, Conceptual Design of the Sodium-Cooled Fast Reactor Kalimer-600, *Nuclear Engineering and Technology, 39* (2007), 3, pp. 193-206

[13] Cinotti, L., *et al.*, Lead-Cooled System Design and Challenges in the Frame of Generation IV International Forum, *Journal of Nuclear Materials, 415* (2011), 3, pp. 245-253

[14] Smith, C. F., *et al.*, SSTAR: The US lead-cooled fast reactor (LFR), *Journal of Nuclear Materials, 376* (2008), 3, pp. 255-259

[15] Holt, M., Andrews, A., Nuclear Power Plants: Vulnerability to Terrorist Attack, Aug. 2007

[16] ***, ACI Committee 349, Code Requirements for Nuclear Safety-Related Concrete Structures (ACI 349-06) and Commentary, American Concrete Institute, Aug. 2007

[17] Ichikawa, T., Koizumi, H., Possibility of Radiation-Induced Degradation of Concrete by Alkali-Silica Reaction of Aggregates, *Journal of Nuclear Science and Technology, 39* (2002), 8, pp. 880-884

[18] Pomaro, B., *et al.*, Radiation Damage Evaluation on Concrete Shielding for Nuclear Physics Experiments, *Ann. Solid Struct. Mech., 2* (2011), 2, pp. 123-142

[19] Edgemon, G. L., Anantatmula, R., Hanford Waste Tnak System Degradation Mechanisms, 1995

[20] Caer, S. Le., Water Radiolysis: Influence of Oxide Surfaces on H2 Production under Ionizing Radiation, *Water, 3* (2011), 4, pp. 235-253

[21] Coderre, J., Principles of Radiation Interactions, July, 2004, pp. 1-17

[22] Hochanadel, C. J., Effects of Cobalt γ-Radiation on Water and Aqueous Solutions, *J. Phys. Chem., 56* (1952), 5, pp. 587-594

[23] Neville, A. M., Properties of Concrete; 5th ed. Harlow England: Pearson, 2011

[24] ***, Portland Cement Association, Portland Cement, Concrete, and Heat of Hydration, *Concrete Technology Today, 18* (1997), 2, pp. 1-8

[25] Abrams, M. S., Compressive Strength of Concrete at Temperatures to 1600F, SP, 25 (1971), Jan., pp. 33-58

[26] William, K., *et al.*, A Review of the Effects of Radiation on Microstructure and Properties of Concretes Used in Nuclear Power Plants., Nov. 2013, pp. 1-131

[27] Boles, M., Cengel, Y., Thermodynamics: An Engineering Approach. McGraw-Hill Education, 2014

[28] Brown, T. D., Javaid, M. Y., The Thermal conductivity of Fresh Concrete, *Mat. Constr., 3* (1970), 6, pp. 411-416

[29] ***, ASTM International, Making and Curing Concrete Test Specimens in the Laboratory, ASTM International, West Conshohocken, 2000

[30] Goorley, J. T., *et al.*, Initial MCNP6 Release Overview – MCNP6 version 1.0, Jun. 2013

[31] ***, Landauer, In Light Complete Dosimetry System Solution, [Online], Available: http://www.landauer.com/uploadedFiles/InLight_nanoDot_FN.pdf. [Accessed: 27-Dec-2015]

[32] ***, Instron, Industrial Series HVL Models, instron.us. [Online]. Available: http://www.instron.us/en-us/products/testing-systems/universal-testing-systems/static-hydraulic/hvl. [Accessed: 01-Apr-2016]

S. Burnham, *et al.*: Effects of Gamma Radiation Induced Forced Formation of ...
Nuclear Technology & Radiation Protection: Year 2017, Vol. 32, No. 4, pp. 307-319

319

[33] ***, ASTM International, Standard Test Method for Compressive Strength of Hydraulic Cement Mortars (Using 2-in. or [50-mm] Cube Specimens), 2002

[34] Hou, D., *et al.*, Morphology of Calcium Silicate Hydrate (C-S-H) Gel: a Molecular Dynamic Study, *Advances in Cement Research, 27* (2015), 3, pp. 135-146

[35] Agostinelli, S., *et al.*, Geant4-a Simulation Toolkit, Nuclear Instruments and Methods in Physics Research Section A: Accelerators, Spectrometers, *Detectors and Associated Equipment, 506* (2003), 3, pp. 250-303

[36] Incerti, S., *et al.*, Comparison of GEANT4 Very Low Energy Cross Section Models with Experimental Data in Water, *Med. Phys., 37* (2010), 9, p. 4692

[37] Bernal, M. A., *et al.*, Track Structure Modeling in liquid Water: A Review of the Geant4-DNA Very Low Energy Extension of the Geant4 Monte Carlo Simulation Toolkit, *Physica Medica, 31* (2015), 8, pp. 861-874

[38] McConn, R. J., *et al.*, Compendium of Material Composition Data for Radiation Transport Modeling, 2011

[39] Hernandez, M. G., *et al.*, Porosity Estimation of Concrete by Ultrasonic NDE, *Ultrasonics, 38* (2000), 1, pp. 531-533

Стивен БУРНАМ, Квентин ФАРЕ, Мишел ТЕМПЛИН, Лонг ХУАН, Татјана ЈЕВРЕМОВИЋ

УТИЦАЈ СТВАРАЊА СЛОБОДНИХ РАДИКАЛА ИНДУКОВАНИХ ГАМА ЗРАЧЕЊЕМ НА ЧВРСТИНУ БЕТОНА ЗА УПОТРЕБУ У НУКЛЕАРНИМ ЕЛЕКТРАНАМА

У овом раду дајемо преглед прелиминарних експеримената и нумеричких процена утицаја стварања слободних радикала под дејством гама зрачења на карактеристике бетона у фази сазревања. Штетни утицаји дуготрајног излагања високим дозама гама и неутронског зрачења бетона обимно су документовани у литератури. Међутим, ми смо показали да краткотрајна излагања бетона гама зрачењу могу бити корисна за повећање његове чврстине на притисак. Извршено је поређење утицаја излагања 56 коцки бетона запремине 125 cm^3, зрачењу ^{137}Cs активности 630 MBq, током првих седам дана сазревања и 56 коцки подвргнутих конвенционалном процесу сазревања. Средња јачина на притисак коцки третираних гама зрачењем је око 8500 psi док је средња јачина на притисак конвенционално третираних коцки износила око 6700 psi. Употребом скенирајућег електронског микроскопа анализирана је микроструктура коцки подвргнутих гама зрачењу и конвенционалном поступку зрења. Радиолиза микроструктура коцки бетона процењена је компјутерским моделовањем применом пакета Geant4. Производња слободних радикала радиолизом расте са повећањем јачине извора и временом излагања гама зрачењу. Ово истраживање показује да, у општем случају, сазревање бетона у пољу гама зрачења даје приметан тренд ка порасту чврстине.

Кључне речи: бетон за нуклеарну индустрију, чврстина бетона, Geant4, гама зрачење